Growth and Properties of Hybrid Organic-Inorganic Metalcone Films Using Molecular Layer Deposition Techniques

*Byoung H. Lee, Byunghoon Yoon, Aziz I. Abdulagatov, Robert A. Hall, and Steven M. George**

Molecular layer deposition (MLD) is a useful technique for fabricating hybrid organic-inorganic thin films. MLD allows for the growth of ultrathin and conformal films using sequential, self-limiting reactions. This article focuses on the MLD of hybrid organic-inorganic films grown using metal precursors and various organic alcohols that yield metal alkoxide films. This family of metal alkoxides can be described as "metalcones". Many metalcones are possible, such as the "alucones" and "zincones" based on the reaction of trimethylaluminum and diethylzinc, respectively, with various organic diols such as ethylene glycol. Alloys of the various metalcones with their parent metal oxide atomic layer deposition (ALD) films can also be fabricated that have an organic-inorganic composition that can be adjusted by controlling the relative number of ALD and MLD cycles. These metalcone alloys have tunable chemical, optical, mechanical, and electrical properties that may be useful for designing various functional films. The metalcone hybrid organic-inorganic materials offer a new tool set for engineering thin film properties.

1. Introduction

Hybrid organic-inorganic materials are useful in a variety of fields including electronics,[1,2] optoelectronics,[3] photonics,[4] protective coatings,[5] catalysis,[6,7] sensors[1,8] and electrochemistry.[9] In general, the inorganic constituent of hybrid organic-inorganic materials can provide desirable mechanical, optical, chemical, and electrical properties. The organic consituent can provide higher flexibility, reduced density, and lower cost. Hybrid materials composed of organic and inorganic components offer the opportunity to develop new materials with tunable properties. These hybrid materials may have synergistic interactions leading to improved performance.

The development of new hybrid organic-inorganic materials is dependent on the methods used to prepare these materials and tune their composition. There are a variety of solution-based approaches for preparing hybrid materials including sol-gel processes,[10,11] Langmuir–Blodgett (LB) techniques,[12,13] layer-by-layer assembly,[14,15] polysilsesquionxane building blocks,[16] and self-assembly procedures.[17,18] Although hybrid films can successfully be fabricated with these solution-based techniques, some benefits could be derived from a gas-phase approach that could control the film thickness and composition at the atomic level and have the ability to coat conformally high aspect ratio structures.

Atomic layer deposition (ALD) techniques have developed rapidly in recent years for many applications.[19] The sequential, self-limiting surface reactions that define the ALD process can deposit conformal ultrathin films with atomic level control on high aspect ratio structures.[20–22] The control of the ALD growth is about 1 Å per reaction cycle and the resulting ALD films have been shown to be continuous and pinhole-free.[23,24] Most ALD techniques are based on binary reaction sequences where two surface reactions occur and deposit a wide range of binary inorganic compounds.[25] The most common ALD materials are metal oxides and metal nitrides. For example, Al_2O_3 ALD is a representative metal oxide that is grown using $Al(CH_3)_3$ and H_2O as the two precursors.[26–28] TiN ALD is a well-studied metal nitride that is grown using $TiCl_4$ and NH_3 as the two precursors.[29,30]

Recently, the types of materials that can be grown using sequential, self-limiting reactions have expanded dramatically with the introduction of organic precursors. Since a molecular fragment can be added to the films, this area is known as "molecular" layer deposition (MLD).[31] **Figure 1** shows a general schematic representation of MLD growth using sequential, self-limiting surface chemistry. The original MLD of organic polymers was achieved using condensation polymerization reactions by a number of Japanese groups in the 1990s.[32–35] MLD growth with bifunctional reactants has subsequently been studied for organic polymers, such as polyamide,[36,37] polyimide,[38] polyurea,[39] polyurethane,[40] polythiourea,[41,42] and polythiolene.[43] The original MLD of organic polymers followed the development of the gas-phase polymer growth technique known as vapor deposition polymerization (VDP).[44]

Dr. B. H. Lee, Dr. B. Yoon, A. I. Abdulagatov, R. A. Hall, Prof. S. M. George
Departments of Chemistry and Chemical Engineering
University of Colorado
Boulder, CO 80309, USA
E-mail: steven.george@colorado.edu

DOI: 10.1002/adfm.201200370

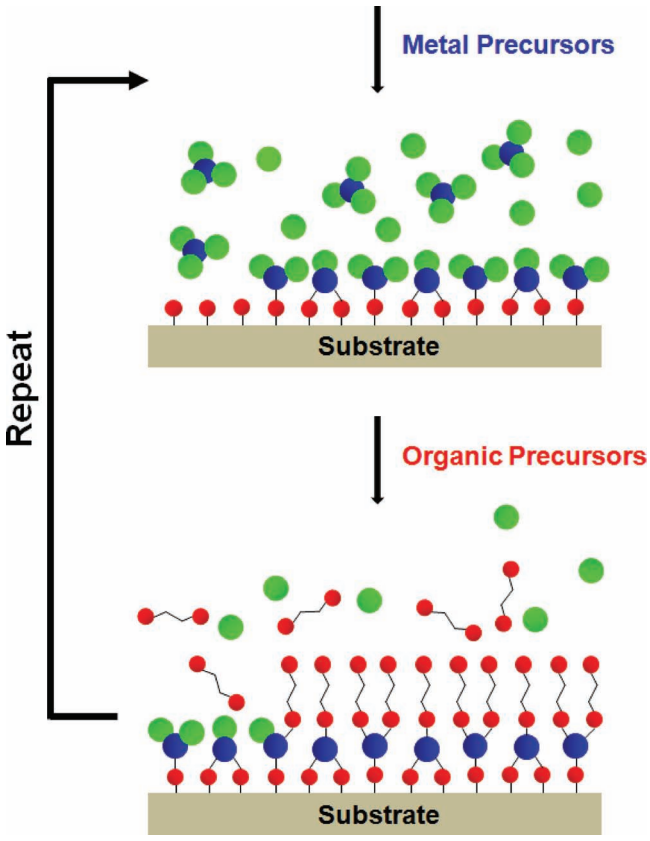

Figure 1. Schematic of MLD growth using sequential, self-limiting surface reactions.

The organic precursors used for all-organic MLD can also be mixed with the inorganic precursors from ALD to define new hybrid organic-inorganic materials.[31] These new systems using organic and inorganic precursors have greatly expanded the possible materials that can be grown using ALD and MLD. In particular, the many kinds of organic precursors available from organic chemistry yield a huge variety of possibilities. One class of hybrid organic-inorganic films is the metal alkoxide films that can be grown from metal precursors and various organic alcohols. These metal alkoxide polymeric films are described as "metalcones".[45] The first metalcones were the "alucones" based on trimethylaluminum (TMA) and ethylene glycol (EG).[46] The "zincones" are another type of metalcone based on diethylzinc (DEZ) and EG.[47,48] The MLD of alucone has also been extended to a three-step ABC reaction sequence using TMA, ethanolamine, and maleic anhydride in order to avoid double reaction problems of homobifunctional reactants.[49,50] A wide variety of other hybrid organic-inorganic films can be deposited using other organic precursors such as carboxylic acids[51,52] or alkylsilanes.[53–56]

Metalcone composites can also be deposited by combining the metalcone MLD process with the parent metal oxide ALD process. The composition of the resulting organic-inorganic film can be controlled by varying the relative number of ALD and MLD cycles. These hybrid organic-inorganic mixtures can be called "metalcone alloys".[45,57] The possibility to mix and match organic and inorganic precursors and their relative contribution in the film leads to a wide spectrum of film properties.[45,57] These metalcone alloys can show tunable properties that vary from hard/dense metal oxides to soft/less dense metal alkoxides. These tunable properties may be valuable for depositing films with varying density, elastic modulus, hardness, refractive index, and dielectric constant.

This feature article will first review the MLD of all-organic polymers such as polyimides and polyamides. The MLD of "alucones" and "zincones" based on aluminum and zinc metal precursors, respectively, and organic diols will then be introduced to illustrate the growth of the metalcone films. Some recent additional metalcones will also be reported based on titanium, zirconium, and hafnium metal precursors known as "titanicones", "zircones", and "hafnicones", respectively. This article will then discuss the growth of metalcone alloys based on metalcone MLD combined with the parent metal oxide ALD. These metalcone alloys have tunable chemical, electrical, optical, and mechanical properties. Lastly, speculations will be offered on the future prospects for the MLD of other metalcone materials and their applications.

2. Organic Polymers Using Molecular Layer Deposition

The first organic polymers grown using MLD techniques were the polyimides[32] and polyamides.[34] This MLD growth

Byoung Hoon Lee received his masters degree in 2007 from Kookmin University and Ph.D. in chemistry in 2010 from Hanyang University. He is currently a postdoctoral research associate at the University of Colorado at Boulder. His research interests are focused on various metalcones and metalcone alloys using atomic and molecular layer deposition for flexible electronic devices.

Steven M. George is a Professor in the Departments of Chemistry and Chemical Engineering at the University of Colorado at Boulder. Dr. George received his B.S. in chemistry from Yale University in 1977 and Ph.D. in chemistry from the University of California Berkeley in 1983. His research interests are in surface chemistry, thin film growth, and nanostructure engineering. He is currently directing a research effort focusing on the development and applications of atomic layer deposition (ALD) and molecular layer deposition (MLD).

employed homobifunctional organic reactants. The surface chemistry was based on stepwise condensation polymerization reactions. The homobifunctional reactants were molecules such as XRX and YR′Y. "X" and "Y" are chemical functional groups, and R and R' are organic fragments. A basic AB reaction with two homobifunctional reactants is:[31]

$$(A)SR'Y* + XRX \rightarrow SR' - RX* + XY \quad (1)$$

$$(B)SRX* + YR'Y \rightarrow SR - R'Y* + XY \quad (2)$$

where the asterisks indicate the surface species. The underlying substrate and deposited film is represented by "S". In the A reaction, the X chemical functionality reacts with SR′Y* species to form SR′-RX* species. In the B reaction, the Y chemical functionality reacts with SRX′ species to form SR-R′Y* species.

Two polyamide MLD systems that have been studied in more detail are nylon 66[37] and poly(*p*-phenylene terephthalamide) (PPTA).[36] Nylon 66 MLD utilized adipoyl chloride (ClOC-$(CH_2)_4$-COCl) (AC) and 1,6-hexanediamine (H_2N-$(CH_2)_6$-NH_2) (HD) as the reactants. The acyl chloride and amine functional groups react to form an amide linkage. In situ Fourier transform infrared (FTIR) measurements explored the surface chemistry and observed linear growth versus the number of AB cycles during nylon 66 MLD.[37] The nylon 66 growth rate was ≈19 Å/cycle.

PPTA MLD has also been investigated using terephthaloyl chloride ($ClCOC_6H_4COCl$) (TC) and *p*-phenylenediamine ($NH_2C_6H_4NH_2$) (PD) as the reactants.[36] The acyl chloride and amine functional groups again react to form amine linkages. In situ FTIR measurements demonstrated that the TC and PD reactions displayed self-limiting surface chemistry and linear growth. However, the linear growth rates were not reproducible from run to run and varied from 0.5 to 3.3 Å per AB cycle.

Polyimide MLD using pyromellitic dianhydride (PMDA) and diamines as the reactants has also been studied by various surface science techniques.[58–60] Electron energy loss investigations monitored the reaction between PMDA and 1,4-phenylene diamine (PDA) and observed the initial formation of amic acid. The amic acid converted to the polyimide with the loss of H_2O. Reflection-absorption infrared spectroscopy was also used to monitor the growth of polyimide using PDMA and 4,4-oxidianiline (ODA) reactants.[59] Studies of polyimide MLD growth have observed temperature-dependent linear growth rates.[38] Polyimide deposited by using PMDA and ODA at 160 °C was consistent with a growth rate of ≈5 Å/cycle.[38]

Polythiourea MLD has been studied using 1,4 phenylene diisothiocyanate and ethylenediamine as reactants.[41,42] Spectroscopic ellipsometry studies showed that the MLD growth is extremely linear versus the number of cycles with a growth rate of 1.9 Å/cycle. FTIR studies demonstrated that the vibrational modes of polythiourea films were consistent with the vibrational spectrum predicted by theoretical density functional theory (DFT). X-ray photoelectron spectroscopy (XPS) measurements also revealed that the composition of the polythiourea films closely matched the expected atomic ratios.

Organic polymer MLD using homobifunctional reactants can face difficulties because both functional groups can react with chemical groups on the surface.[36,37] These "double" reactions subtract reactive sites from the growing polymer surface and inhibit the polymer chain growth. These double reactions can limit the polymer thickness deposited during one AB cycle and lead to irreproducible MLD growth rates.[36,37]

3. Metalcones Using Molecular Layer Deposition

3.1. Alucone MLD Using Trimethylaluminum and Organic Diols and Polyols

Metalcone MLD can be accomplished by combining a metal precursor used in a typical ALD process with an organic precursor used in the MLD of an all-organic polymer.[45] Alucones are one of a number of possible metal alkoxides that define the family of metalcones.[46] The first alucone MLD system was based on the reaction between trimethylaluminum (TMA) and ethylene glycol (EG).[46] The EG molecule, $HO(CH_2)_2OH$, contains two hydroxyls groups and is very similar to H_2O that is used as a reactant in Al_2O_3 ALD.[26,28] The difference is that a $–CH_2–CH_2–$molecular fragment is introduced between the oxygen atoms in the hybrid organic-inorganic film. A schematic showing the growth of the alucone based on TMA and EG is displayed in **Figure 2**.[46]

The general two-step reaction between metal alkyls and diols for metalcone MLD can be written as:[31,46]

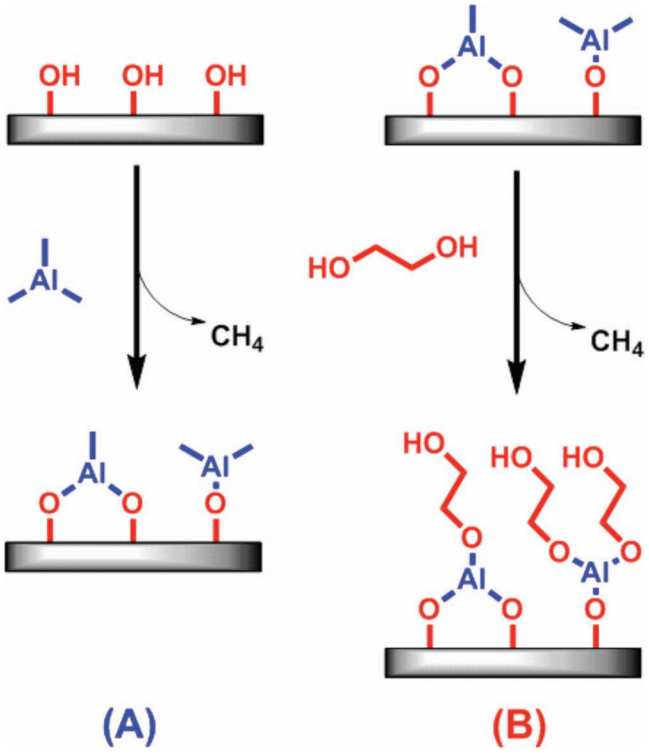

Figure 2. Schematic illustrating alucone MLD film growth using trimethylaluminum (TMA) and ethylene glycol (EG). Reproduced with permission.[31] Copyright 2009, American Chemical Society.

$$(A)SR'OH* + MR_x \rightarrow SR'O - MR_{x-1}* + RH \quad (3)$$

$$(B)SMR* + HOR'OH \rightarrow SM - OR'OH* + RH \quad (4)$$

The asterisks again indicate the surface species and S denotes the substrate with the reaction products from the previous reactions. In the A reaction, the reaction completes when all the SR'OH* species have completely reacted to produce SR'O–MR_{x-1}* species. In the B reaction, the reaction completes when all the SMR* species have completely reacted to produce SM-OR'OH* species. The sequential reactions of TMA and EG forms a metal alkoxide polymeric film with (Al–(O–CH_2–CH_2–O–)) metal alkoxide linkages.[46]

Alucone MLD using TMA and EG has been demonstrated to be very efficient.[46] X-ray reflectivity (XRR) measurements showed that the MLD growth is extremely linear versus the number of TMA and EG cycles. Quartz crystal microbalance (QCM) measurements also demonstrated the linearity of alucone growth versus the number of TMA and EG exposures. The alucone growth rate decreased from 4.0 Å/cycle at 85 °C to 0.4 Å/cycle at 175 °C.[46] The density of these alucone films was independent of the deposition temperature and constant at ≈1.5 g/cm^3.[46] The density of the alucone films is much less than the density of ≈3.0 g/cm^3 for Al_2O_3 ALD films grown at 177 °C.[27]

MLD growth with TMA and EG displayed self-limiting surface reactions. The alucone films were somewhat sensitive to air exposure and showed a contraction of ≈22% over the first 3 days that the films were exposed to ambient.[46] After this contraction, the films were very stable. The alucone films were extremely smooth and conformal when deposited on nanoparticles. The alucone films will lose their organic component under annealing and produce porous Al_2O_3 films.[61,62] These porous Al_2O_3 films from alucone films may have applications in catalysis and gas separations.[63]

Alucone films can also be fabricated using TMA together with organic triols or polyols such as glycerol [$HOCH_2CH(OH)CH_2OH$, (GL)].[64] The growth of these films is again based on the reaction between hydroxyl groups on the alcohol and $AlCH_3$ groups. With more than two hydroxyl groups on the alcohol, there is greater probability that unreacted hydroxyl groups will remain after polyol reactions with $AlCH_3$* surface species. These unreacted hydroxyl groups can produce additional cross-linking between growing polymer chains that can strengthen the alucone film and lead to higher fracture toughness.

In situ FTIR measurements have shown that alucone film growth using TMA and GL is linear versus the number of MLD cycles.[64] In situ QCM measurements also confirmed the linearity of alucone growth with an average mass gain of 41.5 ng/cm^2/cycle at 150 °C. This mass gain of 41.5 ng/cm^2/cycle is consistent with a growth rate of 2.5 Å per cycle.[64] XRR analysis was also consistent with a growth rate of 2.0–2.3 Å/cycle at 150, 170 and 190 °C. The growth rate of 2.3 Å/cycle at 150 °C was consistent with the QCM measurements. The temperature dependence of the growth rate was negligible compared with the temperature dependence observed for alucone films grown using TMA and EG.[46] This minor temperature dependence suggests that there may be less TMA diffusion into the growing MLD film because of more extensive cross-linking.[64]

X-ray reflectivity (XRR) measurements also demonstrated that the alucone films grown using TMA and GL were very stable versus time.[64] In the first week after growth, there was a slight increase in thickness of ≈9%. Subsequently, no changes were observed for measurement times as long as 6 months. Atomic force microscopy (AFM) measurements showed that the surface roughness of the alucone film was only ≈3.5 Å. Recent mechanical testing has also revealed that the alucone films grown using TMA and GL have a higher critical tensile strain for cracking than the MLD films grown using TMA and EG.[64]

3.2. Zincone MLD Using Diethylzinc and Organic Diols

3.2.1. Aliphatic Organic Diols

Diethylzinc (DEZ) is a reactive and useful ALD precursor for ZnO ALD.[65,66] The DEZ precursor can be combined with various organic alcohols to define another class of metalcones. For example, DEZ can react with diols such as EG to produce the zinc alkoxide polymer family that can be called "zincones" as shown in **Figure 3**.[47,48] The growth and film characteristics of zincone MLD and alucone MLD are very similar. In situ Fourier transform infrared (FTIR) measurements observed self-limiting surface reactions during zincone growth using DEZ and EG.[48] The growth rate was also dependent on growth temperature. The growth rates of the zincone varied from 4.0 Å/cycle at 90 °C to 0.25 Å/MLD cycle at 170 °C.[48]

At higher temperatures, the EG precursors were observed to react twice almost exclusively.[48] The double reaction of EG with two $ZnCH_2CH_3$* species did not terminate the zincone

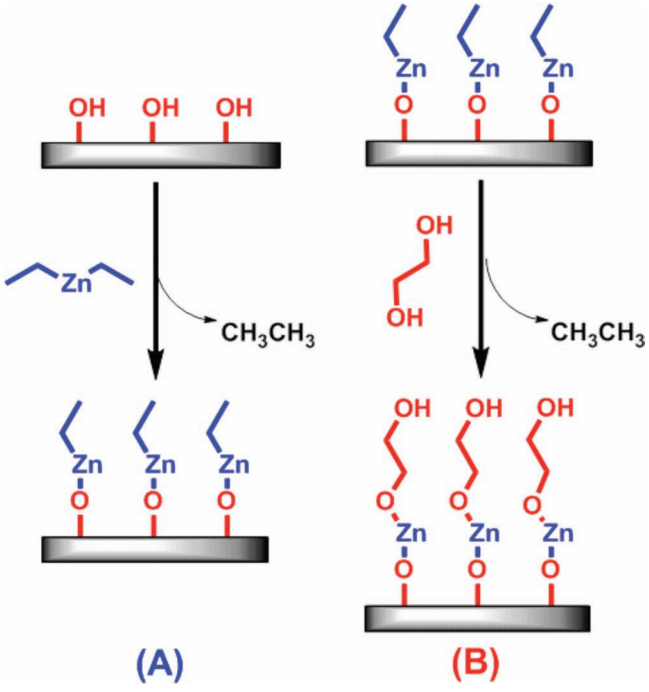

Figure 3. Schematic showing zincone MLD film growth using diethylzinc (DEZ) and ethylene glycol (EG). Reproduced with permission.[48]

film growth at higher temperature. The FTIR spectra suggested that DEZ molecules can diffuse into the MLD film and initiate the growth of new zincone polymer chains. This growth mechanism can also explain the temperature dependence of the zincone growth. At higher temperatures, less DEZ may diffuse into the zincone film. In addition, the DEZ molecules in the zincone film may desorb from the film at a faster rate at higher temperatures. Less diffusion into the film and more desorption of DEZ molecules from the film yields a lower zincone growth per cycle at higher temperatures.[48]

3.2.2. Aromatic Organic Diols

DEZ precursors can also react with aromatic organic diols such as hydroquinone (HQ).[67,68] This new MLD system was examined with the hope that the resulting MLD film would be conductive. Most organic solids are insulators. However, aromatic organics can be electrical conductors resulting from the bands formed by their π and π^* orbitals.[69] The reaction between DEZ and HQ may produce a conjugated chain in the form of (-O-phenyl-O-Zn-)$_n$.[68] Zincone MLD using DEZ and HQ is illustrated in **Figure 4**. The resulting MLD film may be conductive and could have value as a flexible transparent conducting film. In addition, the HQ molecule has a rigid structure based on its aromaticity. This rigid structure is expected to reduce the possibility for double reactions.

In situ QCM measurements showed that the MLD growth was linear versus the number of MLD cycles.[68] The observed mass gains were 28.4 ng/cm^2 for DEZ and 23.9 ng/cm^2 for HQ. The total mass gain was 52.3 ng/cm^2/cycle at 150 °C. XRR measurements also observed that the growth rate was ≈1.6 Å/cycle at 150 °C. The QCM results showed that the DEZ and HQ surface reactions were self-limiting and reached completion after larger DEZ and HQ exposures. The conductance of these zincone films was measured using a four-point probe.[67] The pure zincone films grown using DEZ and HQ showed a low conductivity with a resistivity of 4.4 Ω cm. However, higher conductiviy was observed in alloy systems grown using different relative numbers of zincone MLD and ZnO ALD cycles.[67] These results will be discussed further in Section 4.3.

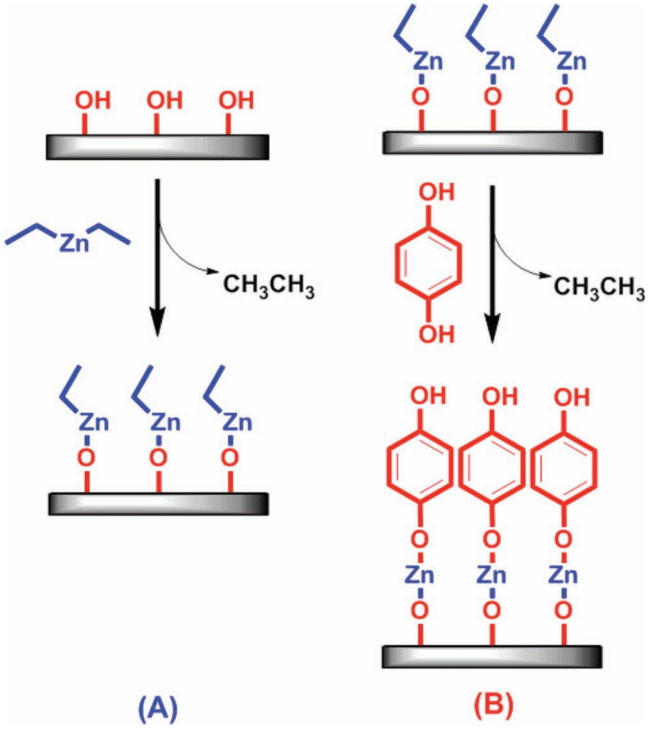

Figure 4. Schematic depicting zincone MLD film growth using diethylzinc (DEZ) and hydroquinone (HQ). Reproduced with permission.[68] Copyright 2011, The Electrochemical Society.

3.2.3. Conjugated Organic Diols

Conjugated organic diols, such as hexadiyne diol (HDD), can also be employed together with DEZ to produce other types of zincone MLD films. Recent work has fabricated two-dimensional polydiacetylene chains bridged by inorganic cross-linkers using MLD techniques at 100–150 °C.[70] The 2D structure of the polydiacetylene chains was obtained by diacetylene polymerization to polydiacetylene during UV exposure. A schematic of the DEZ, HDD, and UV light reaction sequence is shown in **Figure 5**.[70]

The growth rate for the polydiacetylene films with inorganic cross-linkers was determined by spectroscopic ellipsometry and transmission electron microscopy (TEM).[70] Spectroscopic ellipsometry studies also showed that the DEZ and HDD surface reactions were self-limiting and reached completion versus DEG and HDD exposures. The measured growth rate was ≈5.2 Å/cycle.[70] The TEM measurements observed that the MLD films were amorphous. AFM studies also revealed that the films were very smooth. The root mean square roughness of the surfaces was ≈2.5 Å.[70]

These polydiacetylene films with inorganic cross-linkers were used as a semiconductor layer to fabricate thin film transistors (TFTs). These TFTs showed a maximum field effect mobility of 1.3 cm^2/V s with an on/off ratio of ≈10^6 when operating at 100 V.[70] These MLD films may be able to serve as semiconductors with enhanced carrier mobility for flexible electronic device applications.

3.3. Titanicone, Zircone, and Hafnicone MLD

3.3.1. Titanicone MLD Using Titanium Tetrachloride and Organic Diols and Triols

A variety of additional metalcones can be grown using different metal precursors and organic alcohols.[45] Metalcones based on titanium can be fabricated using titanium tetrachloride ($TiCl_4$) and organic alcohols. These titanium-alkoxides can be called "titanicones".[45,71] These titanicone MLD films may have important photocatalytic properties.[72] Titanicones have recently been developed using $TiCl_4$ and EG or GL.[71]

The growth rate for titanicone films using $TiCl_4$ and EG or GL was determined by in situ QCM and ex situ XRR measurements. For titanicone films grown using $TiCl_4$ and EG, the growth rate was ≈83 ng/cm^2/cycle or ≈4.5 Å/cycle from 90–115 °C. For titanicone films grown using $TiCl_4$ and GL, the

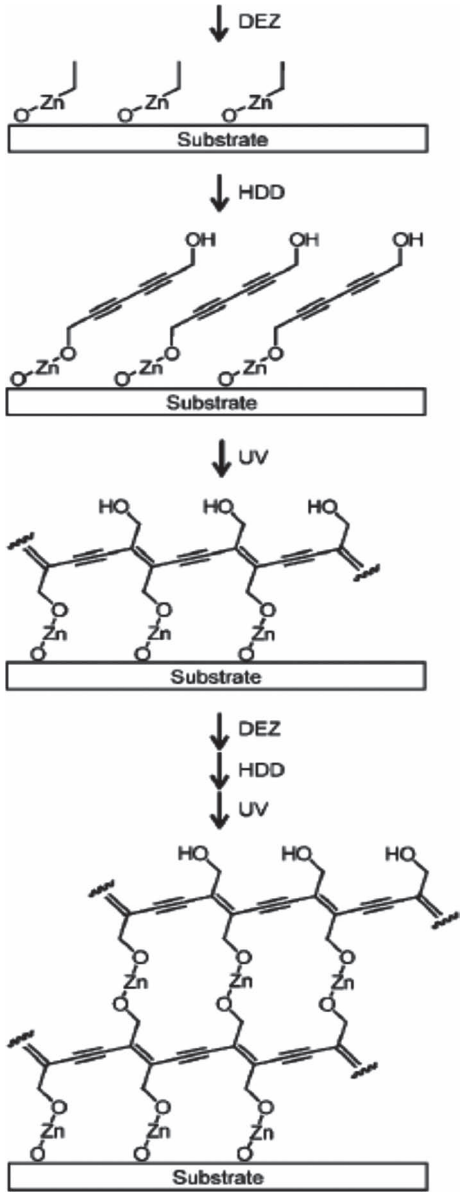

Figure 5. Schematic showing reaction sequence for zinc oxide cross-linked polydiacetylene (ZnOPDA) film. Reproduced with permission.[70]

mass gains obtained at 130–210 °C varied from 48.6 to 33.8 ng/cm^2/cycle, respectively.[71] The growth rate was highest at 2.8 Å/cycle at 130 °C. The low vapor pressure of GL limited the lowest growth temperature to 130 °C.

XRR analysis showed that the titanicone films grown using $TiCl_4$ and GL at 150 °C had higher stability than titanicone films grown using $TiCl_4$ and EG at 115 °C when exposed to air. Nanoindentation experiments also indicated that the elastic modulus and hardness of the titanicone films grown using $TiCl_4$ and GL were much higher than titanicone films grown using $TiCl_4$ and EG.[71] These results are consistent with more cross-linking in the titanicone MLD films grown using $TiCl_4$ and GL. The titanicone films absorbed light in the ultraviolet and the absorption threshold was consistent with an optical bandgap of ≈3.6 eV.

3.3.2. Zircone MLD Using Zirconium Tetra-tert-butoxide and Ethylene Glycol

Zirconium precursors, such as zirconium tetra-tert-butoxide, $Zr[O(C(CH_3)_3)]_4$, can be employed to fabricate another class of metalcone MLD film.[45,73] These hybrid organic-inorganic zirconium alkoxide films can be called "zircones". These zircone MLD films may have interesting dielectric and optical properties because their parent metal oxide, ZrO_2, has a high dielectric constant and a high refractive index.[74,75] **Figure 6** shows the reaction sequence for zircone MLD using ZTB and EG as the reactants.

In situ QCM measurement revealed that the zircone MLD film growth is linear versus the number of MLD cycles.[45,73] The ZTB exposure results in a mass gain of ≈24 ng/cm^2 and the EG exposure results in a mass loss of ≈9 ng/cm^2 at 145 °C.[45] Mass loss is expected when the tert-butoxy ligand is replaced with the alcohol. The mass gain per cycle was ≈15 ng/cm^2/cycle and was very reproducible. The QCM studies also demonstrated that the ZTB and EG surface reactions were self-limiting and reached completion versus ZTB and EG exposures. XRR analysis of the film thickness versus number of MLD cycles was extremely linear and consistent with a growth rate of ≈0.8 Å/cycle at 145 °C.[45,73]

XRR measurements showed that the zircone MLD growth rates decreased at higher temperatures. The growth rates varied from 1.6 Å/cycle at 105 °C to 0.3 Å/cycle at 195 °C. The decrease in the zircone MLD growth rate versus deposition temperature can be partly attributed to double reactions for EG. The measured zircone film densities were independent of the deposition temperature and constant at ≈2.17 g/cm^3.[45] These measured densities are much less than the density of ≈4 g/cm^3 for pure ZrO_2 ALD films. The XRR measurements also revealed that the zircone MLD films grown using ZTB and EG were very stable.

3.3.3. Hafnicone MLD Using Tetrakis(dimethylamido)hafnium and Ethylene Glycol

Another class of metalcone MLD films are the "hafnicones" based on the reaction of tetrakis(dimethylamido)hafnium (TDMAH) and EG.[45,76] These hafnicone MLD films may also have interesting dielectric and optical properties because their parent metal oxide, HfO_2, has a high dielectric constant and a high refractive index. QCM measurements showed the linearity of hafnicone MLD growth versus TDMAH and EG exposures at 145 °C.[76] XRR measurements also demonstrated that the hafnicone MLD growth is extremely linear versus the number of MLD cycles at 145 °C.[76]

The hafnicone MLD growth rate decreased from 1.2 Å/cycle at 105 °C to 0.4 Å/cycle at 205 °C.[76] The temperature dependence of hafnicone MLD growth is similar to other metalcones using EG as the reactant. The measured density of hafnicone MLD film was independent of the deposition temperature and constant at ≈3.0 g/cm^3.[76] The XRR measurements also revealed that the hafnicone MLD films grown using TDMAH and EG were very stable. Spectroscopic ellipsometry measurements

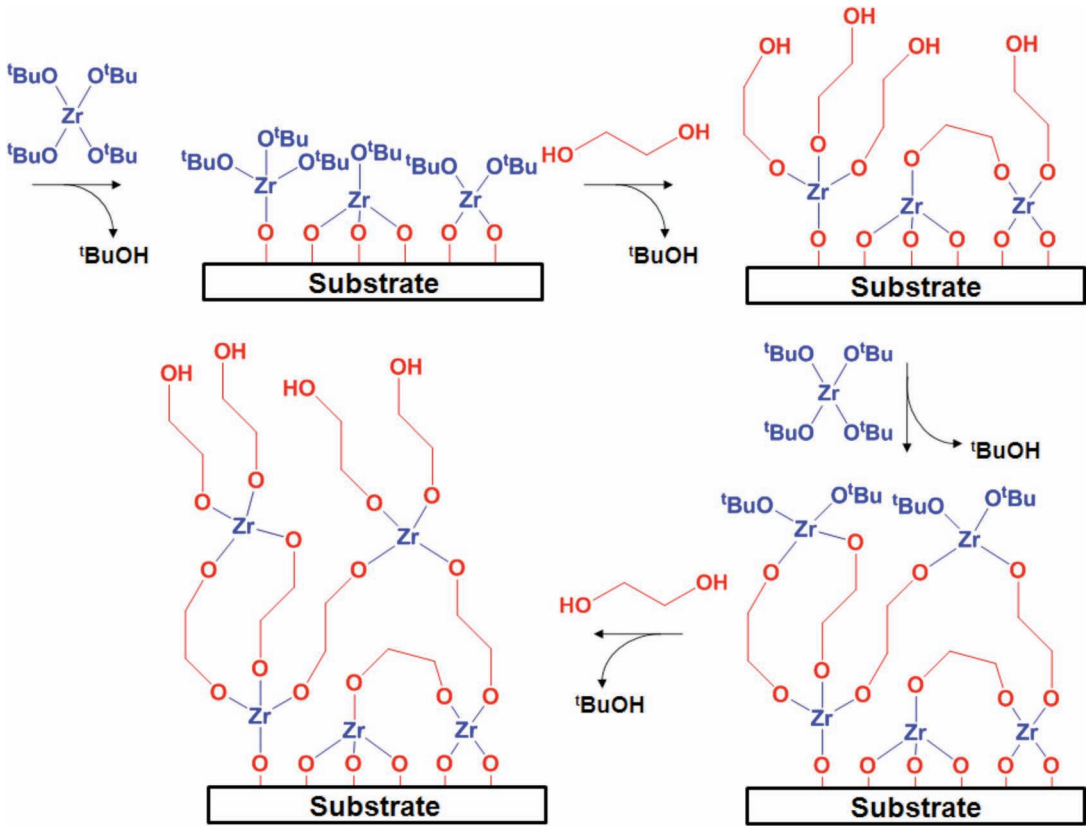

Figure 6. Schematic illustrating zircone MLD film growth using zirconium tetra-tert-butoxide (ZTB) and ethylene glycol (EG). Reproduced with permission.[73] Copyright 2011, The Electrochemical Society.

showed that the refractive index of the hafnicone MLD film was $n = 1.6$.[76] In contrast, HfO_2 ALD films displayed a much higher refractive index of $n = 2.1$.[76]

4. Tunable Metalcone Alloys Using MLD and ALD

4.1. Growth and Tunable Properties of Alucone Alloys

By varying the relative fraction of organic and inorganic constituents, hybrid organic-inorganic polymers can provide a wide range of tunable properties. The hybrid organic-inorganic MLD films have a low density that approaches the low density of organic polymers. In comparison, the inorganic ALD films have a much higher density. Alloys can be grown using metalcone MLD systems and their parent metal oxide ALD systems. These alloys can have a tunable density that varies from the low density of the pure MLD film to the high density of the inorganic ALD film.[45,57] Intermediate densities can be obtained by varying the relative number of ALD and MLD cycles used to grow the alloy film. In addition to density, other parameters can be varied such as elastic modulus, hardness, dielectric constant, refractive index, and conductivity.

Alucone alloys were grown by combining Al_2O_3 ALD and alucone MLD at 135 °C.[45,57] The chemical composition of the alucone alloy was defined by the relative number of the TMA/H_2O ALD cycles and the TMA/EG MLD cycles. For example, the 1:1 alucone alloy was grown using an alternation of the 1 cycle of Al_2O_3 ALD and 1 cycle of alucone MLD. A schematic of the reaction sequence of TMA/H_2O/TMA/EG for the 1:1 alucone alloy is shown in **Figure 7**. In contrast, the 1:2 alucone alloy was grown using an alternation of 1 cycle of Al_2O_3 ALD and 2 cycles of alucone MLD. The reaction sequence for the growth of 1:2 alucone alloy is TMA/H_2O/TMA/EG/TMA/EG.

Figure 8 displays the QCM measurements during the growth of the 1:1 alucone alloy at 135 °C.[57] Mass gains of +12, –1, +10, and +10 ng/cm^2 are obtained during the TMA, H_2O, TMA, and EG exposures, respectively. The 1:1 alucone alloy showed a growth rate of ≈30 ng/cm^2/sequence. The thickness of the 1:1 alucone alloy was also measured using ex situ XRR analysis. The growth rate is ≈3.1 Å/sequence for the 1:1 alucone alloy. These results indicate that the growth of alucone alloy is extremely linear at 135 °C.

Figure 9 shows a cross-sectional transmission electron microscopy (TEM) image of an Al_2O_3 ALD/1:1 alucone alloy/Al_2O_3 ALD trilayer deposited on a Si(100) substrate at 135 °C.[57] The 1:1 alucone alloy film was deposited using 20 TMA/H_2O/TMA/EG sequences. The 1:1 alucone alloy is conformally deposited on the Al_2O_3 ALD layer. The contrast between the Al_2O_3 layers and the 1:1 alucone alloy layer is caused by the lower density of the 1:1 alucone alloy layer. The interfaces between the Al_2O_3

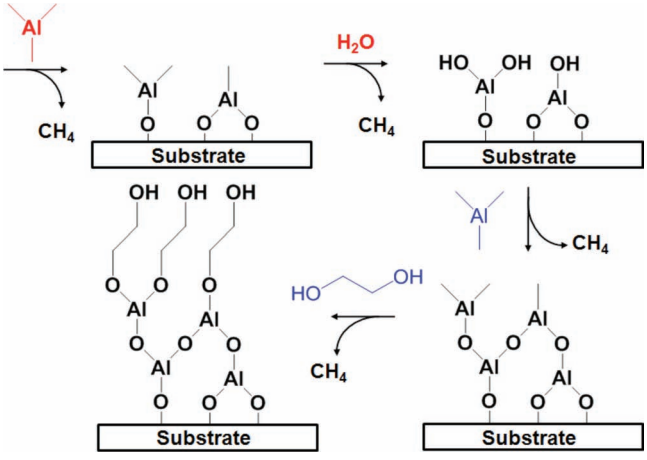

Figure 7. Schematic depicting 1:1 alucone alloy film growth with Al_2O_3 ALD and alucone MLD using TMA and EG. Reproduced with permission.[57] Copyright 2012, American Chemical Society.

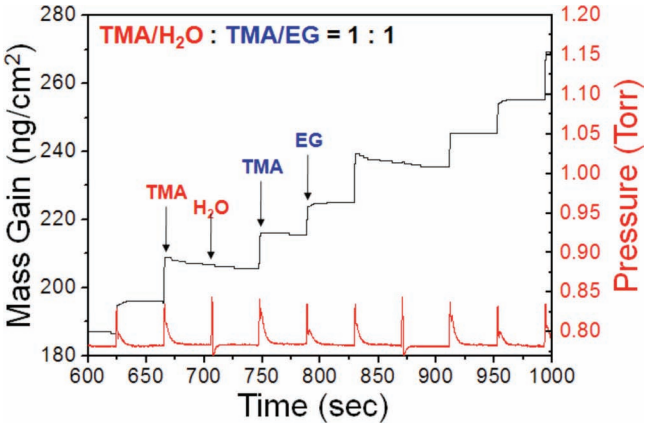

Figure 8. QCM measurements of mass gain and reactor pressure during growth of 1:1 alucone alloy in steady state regime at 135 °C. Reproduced with permission.[57] Copyright 2012, American Chemical Society.

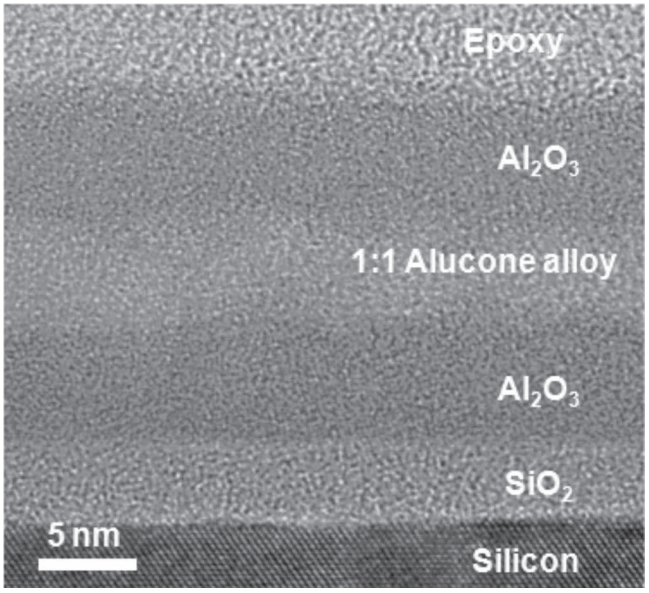

Figure 9. TEM image of 1:1 alucone alloy film sandwiched between two Al_2O_3 ALD films. Reproduced with permission.[57] Copyright 2012, American Chemical Society.

layers and the 1:1 alucone alloy layer are very smooth. The total thickness of the 1:1 alucone alloy layer is ≈6.1 nm. The measured thickness is consistent with the growth rate of ≈3.1 Å/sequence for the 1:1 alucone alloy.

Figure 10a presents the electron density values for alucone alloys grown with different ratios of ALD and MLD cycles.[57] The values were derived from XRR analysis of the alucone alloys. The critical angle, Θ_c, of the XRR scans is related to the electron density, N_e, by $N_e = (\Theta_c^2\pi)/(\lambda^2 r_e)$ where λ is the X-ray wavelength and r_e is the classical electron radius.[77] The mass density, ρ_m, can be related to the electron density by $\rho_m = (N_e A)/(N_A Z)$ where A is the average molar mass, Z is the average atomic number, and N_A is Avogadro's number. A determination of ρ_m from the electron density requires knowledge of the film composition.

The electron densities vary from 5.0×10^{23} e^-/cm^3 for pure alucone MLD films to 8.9×10^{23} e^-/cm^3 for pure Al_2O_3 ALD films.[57] Assuming compositions of -$AlO(CH_2)_2O$- for alucone MLD and Al_2O_3 for Al_2O_3 ALD, the mass densities of the pure alucone MLD film and Al_2O_3 ALD film are 1.6 and 3.0 g/cm^3, respectively. These mass densities are in excellent agreement with previous measurements of 1.5 g/cm^3 for alucone MLD films and 3.0 g/cm^3 for Al_2O_3 ALD films.[46] For the alucone alloys, the mass density increases for higher ALD:MLD ratios during the alloy growth. This result demonstrates that the density of the alucone alloy films can be precisely tuned by changing the relative number of ALD and MLD cycles during the film growth.

Other physical properties that depend on the film density will be changed accordingly. Optical and mechanical properties should vary with composition of the alucone alloy. Figure 10b shows refractive indices obtained from spectroscopic ellipsometry measurements.[57] The refractive indices change from n = 1.45 for pure alucone MLD films to n = 1.64 for pure Al_2O_3 ALD films. The refractive index increases gradually with increasing fraction of Al_2O_3 ALD cycles during film growth. This change is expected based on the relationship between density and refractive index given by the Lorenz-Lorentz equation.[78]

The elastic modulus and hardness of the alucone alloy films were also obtained from nanoindentation measurements.[57] **Figure 11** shows the load versus displacement curves for the pure alucone MLD film, various alucone alloy films and the pure Al_2O_3 ALD film. The elastic modulus and hardness are derived from these load versus displacement curves and evaluated according to the Oliver-Pharr method.[79,80]

Figure 12a shows the elastic modulus for alucone alloys grown with different ratios of ALD and MLD cycles.[57] In agreement with previous measurements,[81,82] the elastic modulus of the pure alucone MLD film and pure Al_2O_3 ALD film are E = 21 ± 8 GPa and E = 198 ± 8 GPa, respectively. The elastic modulus progressively increases for the 1:3, 1:1, and

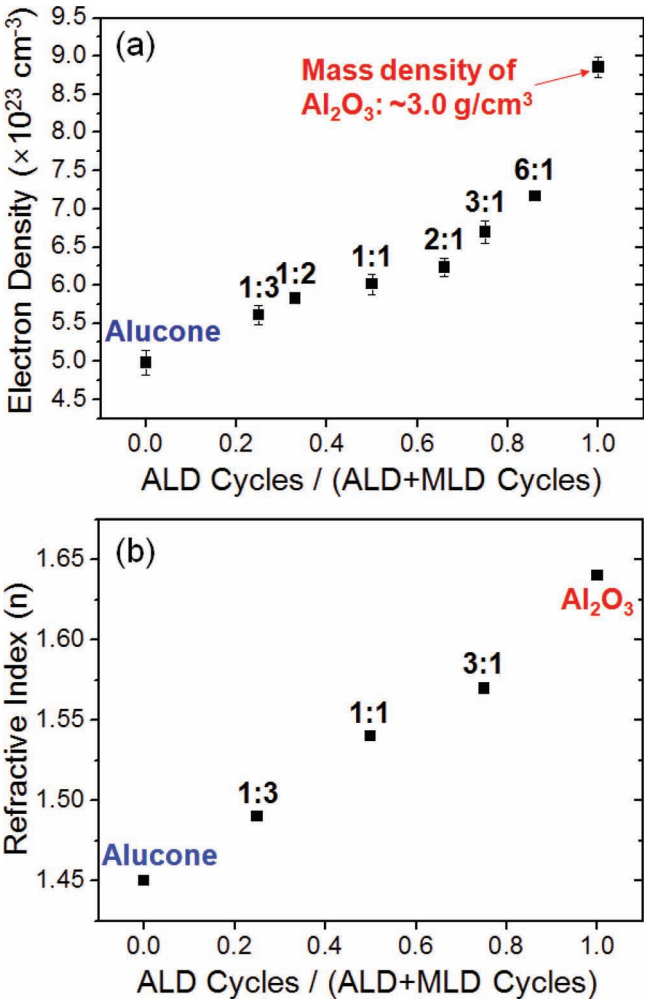

Figure 10. a) Electron density and b) refractive index for Al_2O_3 ALD, alucone MLD and alucone alloys grown with various ALD:MLD ratios. The results are plotted versus the fraction of ALD cycles in the reaction sequence. Reproduced with permission.[57] Copyright 2012, American Chemical Society.

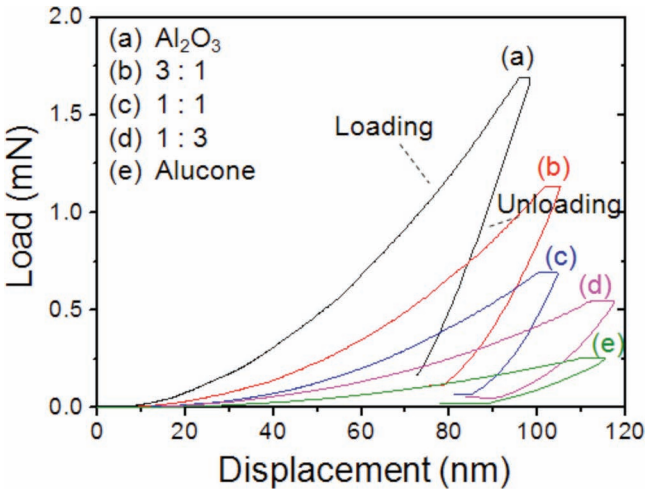

Figure 11. Nanoindentation measurements showing load versus displacement curves for Al_2O_3 ALD, alucone MLD and alucone alloy films grown with ALD:MLD cycle ratios of 3:1, 1:1, and 1:3. Reproduced with permission.[57] Copyright 2012, American Chemical Society.

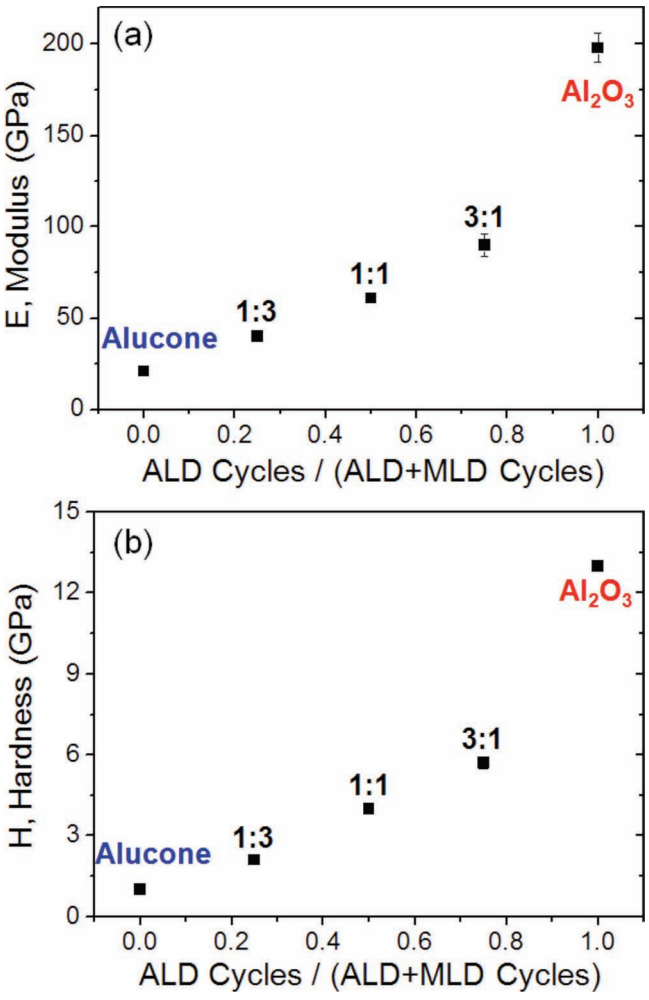

Figure 12. a) Elastic modulus and b) hardness for Al_2O_3 ALD, alucone MLD and alucone alloys grow with ALD:MLD cycle ratios of 3:1, 1:1, and 1:3. Reproduced with permission.[57] Copyright 2012, American Chemical Society.

3:1 alucone alloys before increasing more dramatically to E = 198 ± 8 GPa for the pure Al_2O_3 ALD film. The magnitude for the elastic modulus is higher for larger Al_2O_3 fractions in the alucone alloy films.

Figure 12b displays the hardness for alucone alloys grown with different ratios of ALD and MLD cycles. The hardness of the pure alucone MLD film and pure Al_2O_3 ALD film are H = 1.0 ± 0.1 GPa and H = 13.0 ± 0.2 GPa, respectively. These values agree with previous measurements.[81,83] The hardness progressively increases for the 1:3, 1:1, and 3:1 alucone alloys. The hardness then increases more dramatically to H = 13.0 ± 0.2 GPa for the pure Al_2O_3 ALD film. In similarity to the elastic modulus, the magnitude for the hardness is higher for larger Al_2O_3 fractions in the alucone alloy films.

To investigate the stability of the alucone alloys in air, films grown with different ALD:MLD ratios were deposited on Si substrates. A pure alucone MLD film with a thickness of

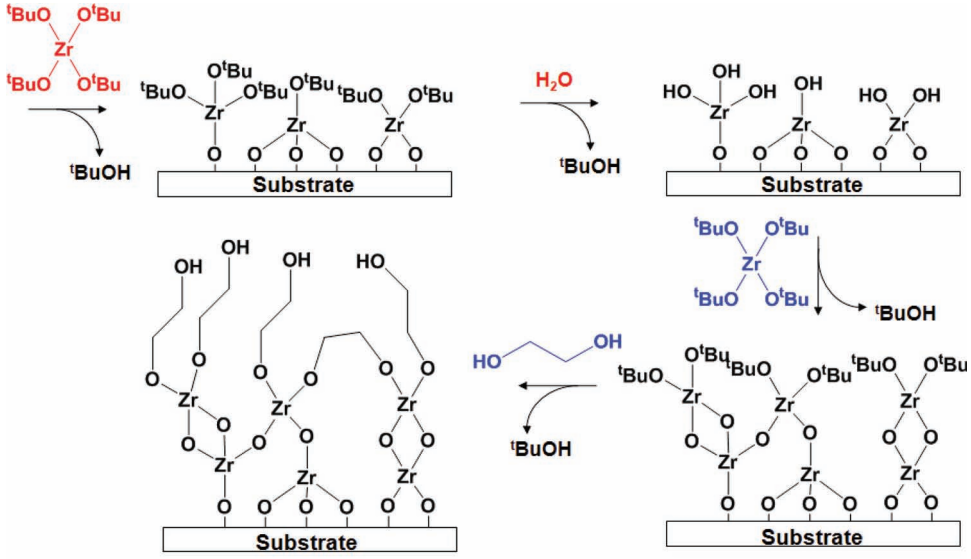

Figure 13. Schematic showing 1:1 zircone alloy film growth with ZrO_2 ALD and zircone MLD using ZTB and EG.

32 nm decreased ≈23% during the first week. This decrease is consistent with previous studies of alucone MLD film stability.[46] A 1:3 alucone alloy film with a thickness of 78 nm also decreased ≈7% after one week. In contrast, no thickness change was observed for the 1:1 and 3:1 alucone alloy films. These results reveal that alucone alloy films containing a higher proportion of Al_2O_3 ALD cycles are stable. The Al_2O_3 fraction in the alucone alloys helps prevent any chemical changes that can lead to film shrinkage.[46]

4.2. Growth and Tunable Properties of Zircone Alloy

Zircone alloys can be grown using zircone MLD and ZrO_2 ALD.[73] Zircone alloys were deposited by changing the relative number of the ZrO_2 ALD cycles and the zircone MLD cycles at 145 °C. **Figure 13** displays the reaction sequence for the zircone alloy deposited using the alternation of one ZrO_2 ALD cycle and one zircone MLD cycle. In contrast, the 1:2 zircone alloy was grown using an alternation of 1 cycle of ZrO_2 ALD and 2 cycles of zircone MLD. The reaction sequence for the growth of the 1:2 zircone alloy is ZTB/H_2O/ZTB/EG/ZTB/EG.

Figure 14 displays the QCM measurements during the growth of a 1:1 zircone alloy at 145 °C.[73] Mass gains of +27, –11, +24, and –5 ng/cm^2 are obtained during the ZTB, H_2O, ZTB, and EG exposures, respectively. The 1:1 zircone alloy displayed a growth rate of ≈34 ng/cm^2/sequence. The thickness of the 1:1 zircone alloy was also measured using ex situ XRR analysis. The growth rate was ≈2.1 Å/sequence for the 1:1 zircone alloy. The QCM and XRR results showed that the growth of the zircone alloys was extremely linear at 145 °C.

Figure 15a shows the electron density values obtained from XRR analysis of zircone alloys grown with different ratios of ALD and MLD cycles.[73] The electron densities vary from 6.2 × 10^{23} e$^-$/cm^3 for pure zircone MLD films to 1.1 × 10^{24} e$^-$/cm^3 for pure ZrO_2 ALD films. Assuming compositions of -$ZrO(CH_2)_2O$- for zircone and ZrO_2 for ZrO_2, the mass densities of the pure zircone film and ZrO_2 film are 2.17 and 4.0 g/cm^3, respectively. For the zircone alloys, the density increases progressively as the ALD:MLD ratio is increased during film growth.

Optical and mechanical properties should also vary with the composition of the zircone alloy. The refractive indices obtained from spectroscopic ellipsometry measurements are shown in Figure 15b.[76] The refractive indices vary from n = 1.63 for pure zircone MLD films to n = 1.86 for pure ZrO_2 ALD films. The refractive index changes gradually and smoothly with increasing ALD:MLD ratio during film growth. This change is again expected based on the relationship between density and refractive index given by the Lorenz-Lorentz equation.[78]

The elastic modulus and hardness of the zircone alloy films were also obtained from nanoindentation measurements.[76]

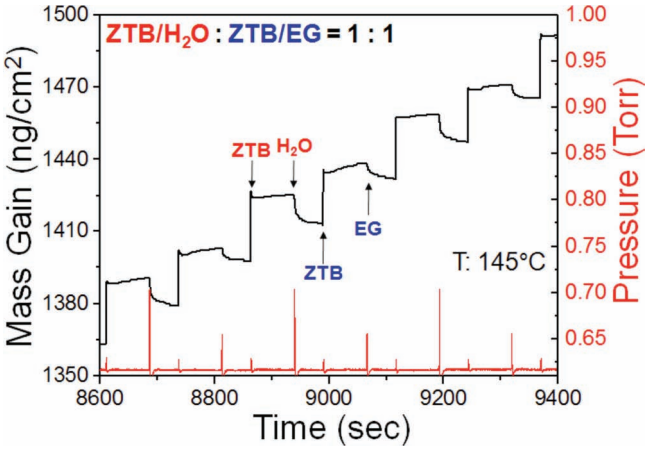

Figure 14. QCM measurements of mass gain and reactor pressure during growth of 1:1 zircone alloy in steady state regime at 145 °C. Reproduced with permission.[73] Copyright 2011, The Electrochemical Society.

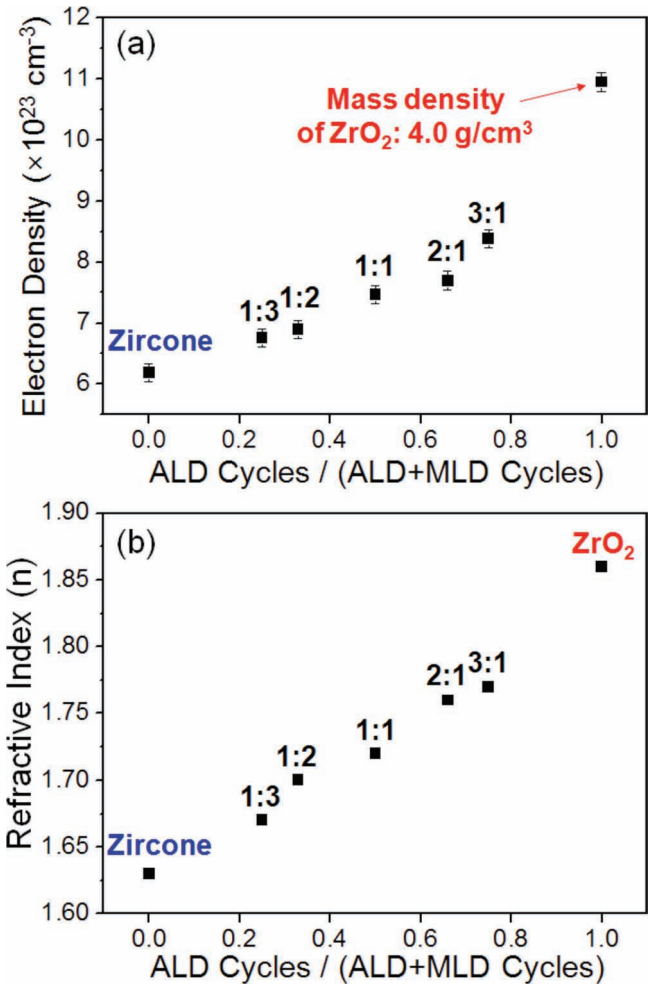

Figure 15. a) Electron density and b) refractive index for ZrO_2 ALD, zircone MLD, and zircone alloys grown with various ALD:MLD ratios. Panel (a) reproduced with permission.[73] Copyright 2011, The Electrochemical Society.

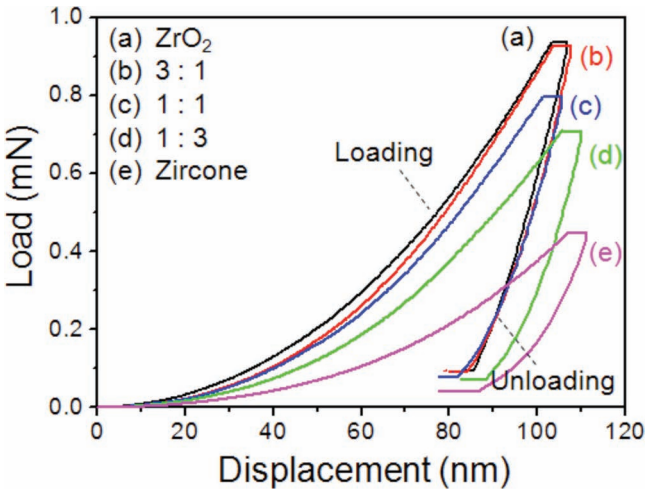

Figure 16. Nanoindentation measurements showing load versus displacement curves for ZrO_2 ALD, zircone MLD and zircone alloy films grown with ALD:MLD cycle ratios of 3:1, 1:1, and 1:3.

Figure 16 shows the load versus displacement curves for the pure zircone MLD film, various zircone alloy films and the pure ZrO_2 ALD film. The elastic modulus and hardness are derived from these load versus displacement curves and evaluated according to the Oliver-Pharr method.[79,80]

Figure 17a shows the elastic modulus for zircone alloys grown with different ratios of ALD and MLD cycles. The elastic modulus of the pure zircone MLD film and pure ZrO_2 ALD film are $E = 27 \pm 0.6$ GPa and $E = 97 \pm 5$ GPa, respectively. The elastic modulus gradually increases with increasing ratio of ALD:MLD cycles during film growth. The magnitude for the elastic modulus is higher for larger ZrO_2 portions in the zircone alloy films.

Figure 17b also displays the hardness for zircone alloys grown with different ratios of ALD and MLD cycles. The hardness of the pure zircone MLD film and pure ZrO_2 ALD film are $H = 1.8 \pm 0.1$ GPa and $H = 4.8 \pm 0.4$ GPa, respectively. The hardness gradually increases with increasing ratio of ALD:MLD cycles during film growth. In similarity to the elastic modulus, the magnitude for the hardness is higher for larger ZrO_2 portions in the zircone alloy films.

4.3. Conductive Zincone Alloy

As discussed in Section 3.2.2, zincone MLD films can be fabricated using DEZ as a zinc metal precursor and hydroquinone (HQ) as an aromatic organic molecule.[67,68] These films may be conductive because of their π-electron conjugation. However, the zincone MLD films grown using DEZ and HQ were not consistently conducting.[68] These results suggested that impurities in the MLD film may be affecting the conductivity. In particular, the presence of H_2O was suspected as a possible problem during zincone MLD with DEZ and HQ.[68]

Zincone alloy films grown using ZnO ALD and zincone MLD may produce a film with a higher conductivity than zincone MLD by itself.[67] Various alloy systems were examined with the hope that the resulting zincone alloy film would display enhanced conductivity. A four-step sequence for the 1:1 zincone alloy film using DEZ, H_2O, DEZ, and HQ is shown in **Figure 18**. The reaction between DEZ, H_2O, DEZ, and EG should yield a chain in the form of $(–O–Zn–O–phenyl–O–Zn–O–)_n$. The resulting zincone alloy films may be conductive because of electron overlap between the π-electrons in the HQ ring and the ZnO moieties.

Figure 19 shows in situ QCM measurements for the growth of the 1:1 zincone alloy. These results show that the zincone alloy film growth is linear. The observed mass gains for this reaction sequence at 150 °C are 24 ng/cm^2 for DEZ, 3 ng/cm^2 for H_2O, 22 ng/cm^2 for the second DEZ and 27 ng/cm^2 for HQ. The total mass gain was 76 ng/cm^2/sequence at 150 °C. The QCM results also demonstrated that the four surface reactions were self-limiting and reached completion during DEZ, H_2O, DEZ, and HQ exposures.

Various zincone alloy films were deposited by varying the number of ZnO ALD cycles and zincone MLD cycles in the

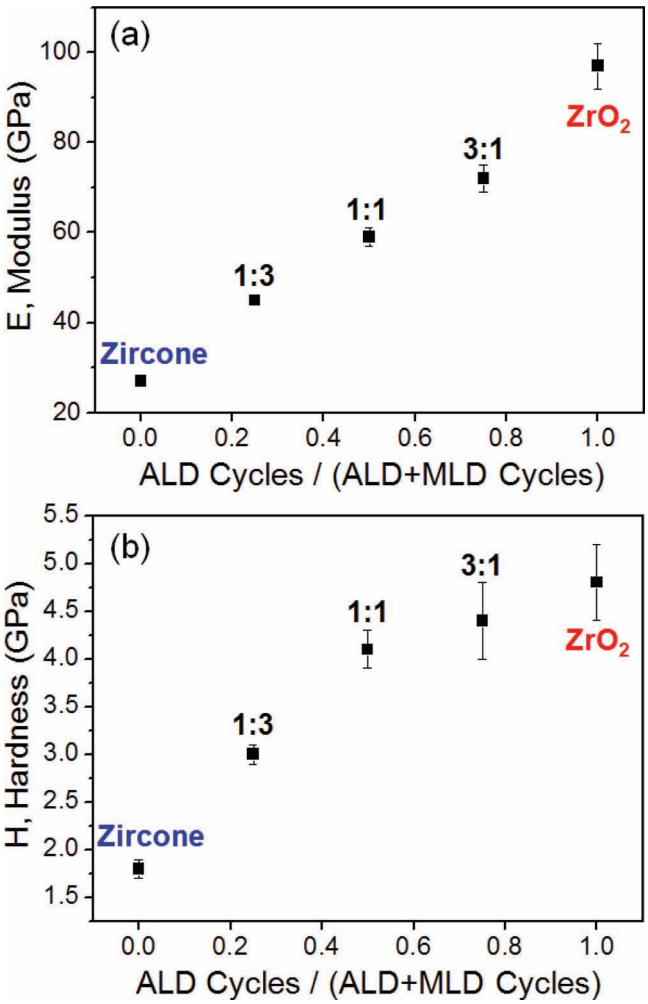

Figure 17. a) Elastic modulus and b) hardness for ZrO_2 ALD, zircone MLD and zircone alloys grown with ALD:MLD cycle ratios of 3:1, 1:1, and 1:3.

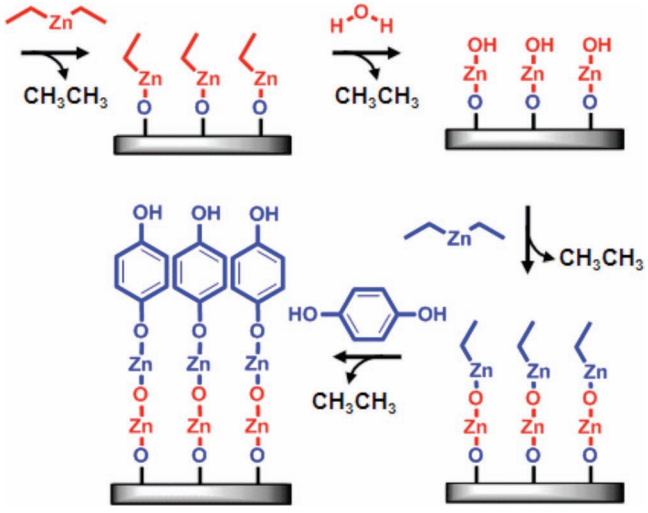

Figure 18. Schematic depicting 1:1 zincone alloy film growth with ZnO ALD and zincone MLD using DEZ and HQ.

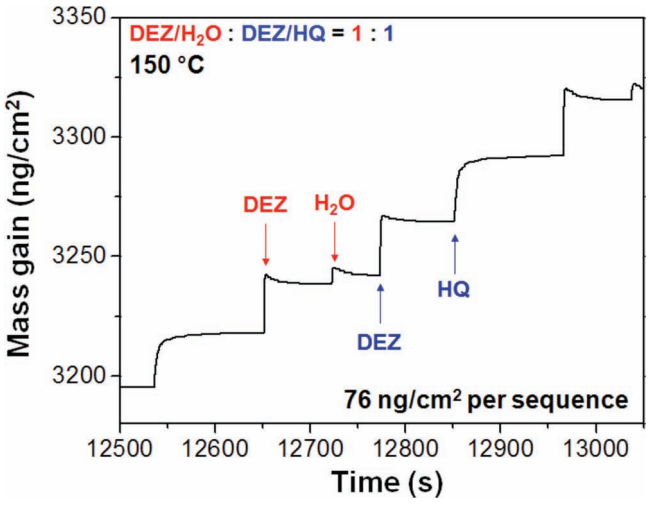

Figure 19. QCM measurements of mass gain during 1:1 zincone alloy growth with ZnO ALD and zincone MLD using DEZ and HQ in steady state regime at 150 °C.

reactant sequence. For example, the 1:3 zincone alloy was grown using the alternation of one cycle of DEZ/H_2O ALD and three cycles of DEZ/HQ MLD. The 2:2 zincone alloy was grown using the alternation of two cycles of DEZ/H_2O ALD and two cycles of DEZ/HQ MLD. The various zincone alloys were then characterized using four-point probe measurements.

Four-point probe electrical measurements for the 2:2 zincone alloy are shown in **Figure 20**. The 2:2 zincone alloy film was fabricated using 1,000 sequences of 2×(DEZ/H_2O)/2×(DEZ/HQ) on non-conductive SiO_2/Si wafers at 150 °C. This zincone alloy film had a thickness of 184 nm measured by X-ray reflectivity (XRR). Figure 20 reveals that the 2:2 zincone alloy film has a higher electrical conductance than a ZnO ALD film with a comparable thickness of 166 nm.

High electron conductivities were consistently observed for zincone alloy films grown using different combinations of ZnO ALD and zincone MLD cycles.[67] **Table 1** shows the observed resistivities for the various zincone alloys. Zincone alloys with ALD:MLD ratios of 1:1, 2:2, and 1:3 all have resistivities lower than ZnO ALD films. The resistivity of ZnO ALD films is 6.9×10^{-2} Ω cm. This resistivity is consistent with previous ZnO conductivity studies.[84] The resistivities for the zincone alloys are in the 10^{-3} Ω cm range. This range is comparable to the Al-doped ZnO thin films.[84,85] These results indicate that zincone alloys can be fabricated with high electron conductivity that may be possible candidates to replace indium tin oxide (ITO) and have applications for flexible and conducting thin films for displays.

5. Conclusions and Future Prospects

Hybrid organic-inorganic films known as metalcones can be deposited using gas phase MLD processing with typical metal ALD precursors and organic alcohols. These metal alkoxides can be grown using sequential surface reactions that allow the films to be deposited conformally with atomic layer control. A wide variety of metalcones have been demonstrated such as alucones,

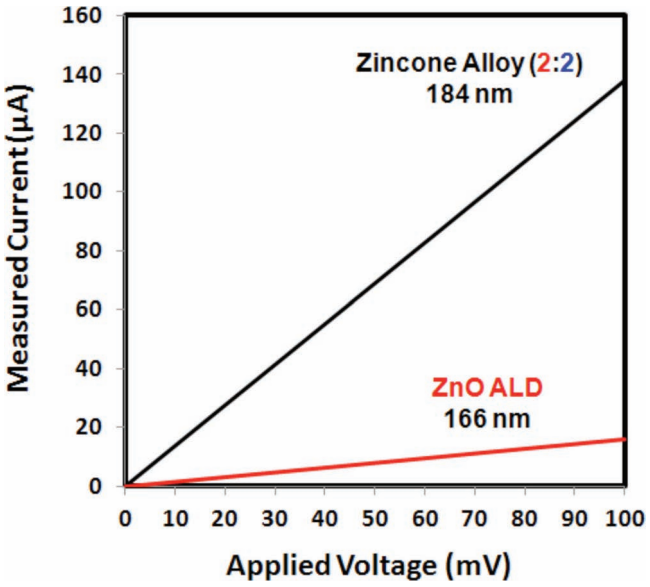

Figure 20. Measured current versus applied voltage for a ZnO ALD film and a 2:2 zincone alloy film grown with ZnO ALD and zincone MLD using DEZ and HQ.

Table 1. Resistivity of ZnO ALD films, zincone MLD films using DEZ, H_2O, and HQ and zincone alloy films grown with ZnO ALD and zincone MLD using DEZ, H_2O, and HQ. Resistivities were obtained using four-point probe measurements.

Films	Thickness [nm]	Resistivity [Ω cm]
ZnO ALD	166	6.9×10^{-2}
Zincone alloy (1:1)	140	8.6×10^{-3}
Zincone alloy (2:2)	184	5.9×10^{-3}
Zincone alloy (1:3)	237	1.2×10^{-2}
Al_2O_3:ZnO (1:1)	200	Non-conductive

zincones, titanicones, zircones and hafnicones. Metalcone alloys can also be deposited by combining metal oxide ALD and metalcone MLD processing. A compilation of the growth rate, density, refractive index, and elastic modulus for the various metalcones and metalcone alloys is given in **Table 2**.

Many other metal precursors could be used to form hybrid organic-inorganic films. The possibilities are extensive given the many metals on the periodic table and organic precursors available from organic chemistry. A summary of the demonstrated metalcones and other potential metalcones are given in **Table 3**. The possible inorganic precursors and the parent metal oxides are given in Table 3. The metal oxide can also be produced from the metalcone by removing the organic constituents using thermal annealing or chemical processing.[61,62] The resulting metal oxide may also have a high porosity.[62] These various metalcones and porous metal oxides formed from the metalcones may have a number of possible applications.

Some zincones have electrical conductivity that may be useful for flexible transparent conducting displays.[67,68] The titanicones or porous TiO_2 scaffolds fabricated from the titanicones may be utilized for photocatalysis or solar cell applications.[72,86] The zircones and hafnicones have high dielectric constants and refractive indices that may be useful for flexible electrical and optical thin film devices.[74,75] The tincones and indicones or porous films derived from tincones and indicones may have properties that could be useful for gas sensors.[87,88] The vanadicones and manganesicones or porous architectures formed using vanadicones and manganesicones may have catalytic and redox activity that could be utilized for catalysis and electrochemical applications.[89,90]

The metalcone alloy films also have tunable mechanical, optical, dielectric, conductive, and chemical properties that should be useful for a variety of applications. For example, the tunable density and refractive index of metalcone alloys could be employed to fabricate films with a graded refractive index for antireflection coatings.[91] The tunable composition of organic and inorganic constituents in the metalcone alloy may be useful for flexible gas diffusion barriers.[92,93] Metalcone alloys could

Table 2. Compilation of the growth rate, density, refractive index, and elastic modulus for the various metalcones and metalcone alloys. TMA = trimethylaluminum, EG = ethylene glycol, GL = glycerol, DEZ = diethylzinc, HQ = hydroquinone, TTC = titanium tetrachloride, ZTB = zirconium tetra-tert-butoxide, TDMAH = tetrakis(dimethylamido)hafnium.

Metalcone	Reactants	Growth Rate [Å/cycle] or [Å/sequence]	Density [g/cm^3]	Refractive Index	Elastic Modulus [GPa]	Ref.
Alucone	TMA, EG	4.0 (85 °C), 0.4 (175 °C)	1.5	1.45	21	[46]
Alucone	TMA, GL	2.0–2.3 (150–190 °C)	1.7	1.54	32	[45,64]
Alucone Alloy	TMA, H_2O, EG	3.1 (1:1, 135 °C)	1.5 (Alucone) -3.0 (Al_2O_3)	1.45 (Alucone) -1.64 (Al_2O_3)	21 (Alucone) -198 (Al_2O_3)	[57]
Zincone	DEZ, EG	4.0 (90 °C), 0.25 (170 °C)	1.9			[48]
Zincone	DEZ, HQ	1.6 (150 °C)	2.0		28	[68]
Zincone Alloy	DEZ, H_2O, HQ	1.5 (1:1, 150 °C)	2.0 (Zincone) - 5.4 (ZnO)		28 (Zincone) -148 (ZnO)	[67]
Titanicone	TTC, EG	4.5 (90–115 °C)	1.8	1.7	8	[45,71]
Titanicone	TTC, GL	2.8 (130 °C), 2.1 (210 °C)	1.8 (130 °C) -1.98 (210 °C)	1.8	30.6	[45,71]
Zircone	ZTB, EG	1.6 (105 °C), 0.3 (195 °C)	2.17	1.63	27	[45,73]
Zircone Alloy	ZTB, H_2O, EG	2.1 (1:1, 145 °C)	2.17 (Zircone) -4.0 (ZrO_2)	1.63 (Zircone) -1.86 (ZrO_2)	27 (Zircone) -97 (ZrO_2)	[73,76]
Hafnicone	TDMAH, EG	1.2 (105 °C), 0.4 (205 °C)	3.0	1.61	47	[76]

Table 3. Summary of various metalcones, inorganic precursors to grow the metalcones, and parent metal oxides obtained after removing the organic constituents.

Metalcone	Inorganic Precursor	Parent Metal Oxide
Alucones	Trimethylaluminum	Al_2O_3
Zincones	Diethylzinc	ZnO
Zircones	Zirconium tetra-*tert*-butoxide	ZrO_2
Hafnicones	Tetrakis(dimethylamido) hafnium	HfO_2
Magnesicones	Bis(ethylcyclopentadienyl) magnesium	MgO
Tincones	Tetradimethylaminotin	SnO_2
Indicones	Trimethylindium	In_2O_3
Titanicones	Tetradimethylaminotitanium	TiO_2
Vanadicones	Bis(ethylcyclopentadienyl) vanadium	V_2O_5
Manganesicones	Bis(ethylcyclopentadienyl) manganese	MnO

also be employed to fabricate functionally graded interlayers of organic-inorganic composites to minimize coefficient of thermal expansion (CTE) mismatch between organic polymer and inorganic films.[94,95] In addition, metalcone alloys could be used to tune polymer interlayer mechanical properties in a multilayer barrier to acheive the highest critical tensile strains.[96]

These hybrid organic-inorganic films deposited using MLD and ALD techniques should change some paradigms in thin film growth. Until the advent of the MLD of organic and hybrid organic-inorganic films, ALD processes had been confined to inorganic materials. With the inorganic materials, there is little flexibility to change the thin film properties. In contrast, hybrid organic-inorganic materials deposited using MLD and ALD techniques can be tuned by changing the relative amount of organic and inorganic constituents. This tunability enables the metalcones and the metalcone alloys to serve as a toolset for the engineering of functional films.

Acknowledgements

This research was funded by the National Science Foundation (CHE-1012116) and DuPont Central Research and Development. Additional support was received from the DARPA Center on Nanoscale Science and Technology for Integrated Micro/Nano-Electomechanical Transducers (iMINT), which is supported by the DARPA/MEMS S&T Fundamentals Program (HR0011-06-1-0048). In addition, some of the equipment used in this research was provided by the Air Force Office of Scientific Research.

Received: February 7, 2012
Revised: July 5, 2012
Published online: September 7, 2012

[1] C. R. Kagan, D. B. Mitzi, C. D. Dimitrakopoulos, *Science* **1999**, *286*, 945.
[2] D. B. Mitzi, *Chem. Mater.* **2001**, *13*, 3283.
[3] E. Holder, N. Tessler, A. L. Rogach, *J. Mater. Chem.* **2008**, *18*, 1064.
[4] C. Sanchez, B. Lebeau, F. Chaput, J. P. Boilot, *Adv. Mater.* **2003**, *15*, 1969.
[5] T. P. Chou, C. Chandrasekaran, S. J. Limmer, S. Seraji, Y. Wu, M. J. Forbess, C. Nguyen, G. Z. Cao, *J. Non-Cryst. Solids* **2001**, *290*, 153.
[6] S. Inagaki, S. Guan, Y. Fukushima, T. Ohsuna, O. Terasaki, *J. Am. Chem. Soc.* **1999**, *121*, 9611.
[7] A. P. Wight, M. E. Davis, *Chem. Rev.* **2002**, *102*, 3589.
[8] S. D. Evans, S. R. Johnson, Y. L. L Cheng, T. H. Shen, *J. Mater. Chem.* **2000**, *10*, 183.
[9] A. Walcarius, *Chem. Mater.* **2001**, *13*, 3351.
[10] C. Sanchez, F. Ribot, *New J. Chem.* **1994**, *18*, 1007.
[11] J. Y. Wen, G. L. Wilkes, *Chem. Mater.* **1996**, *8*, 1667.
[12] M. ClementeLeon, B. Agricole, C. Mingotaud, C. J. GomezGarcia, E. Coronado, P. Delhaes, *Langmuir* **1997**, *13*, 2340.
[13] M. ClementeLeon, C. Mingotaud, B. Agricole, C. J. GomezGarcia, E. Coronado, P. Delhaes, *Angew. Chem. Int. Ed.* **1997**, *36*, 1114.
[14] S. W. Keller, H. N. Kim, T. E. Mallouk, *J. Am. Chem. Soc.* **1994**, *116*, 8817.
[15] H. Lee, L. J. Kepley, H. G. Hong, T. E. Mallouk, *J. Am. Chem. Soc.* **1988**, *110*, 618.
[16] D. A. Loy, K. J. Shea, *Chem. Rev.* **1995**, *95*, 1431.
[17] A. Sellinger, P. M. Weiss, A. Nguyen, Y. F. Lu, R. A. Assink, W. L. Gong, C. J. Brinker, *Nature* **1998**, *394*, 256.
[18] N. Tillman, A. Ulman, T. L. Penner, *Langmuir* **1989**, *5*, 101.
[19] S. M. George, *Chem. Rev.* **2010**, *110*, 111.
[20] S. M. George, A. W. Ott, J. W. Klaus, *J. Phys. Chem.* **1996**, *100*, 13121.
[21] M. Ritala, Leskelä, M., J.-P. Dekker, C. Mutsaers, P. J. Soininen, J. Skarp, *Chem. Vap. Deposition* **1999**, *5*, 7.
[22] J. W. Elam, D. Routkevitch, P. P. Mardilovich, S. M. George, *Chem. Mater.* **2003**, *15*, 3507.
[23] P. F. Carcia, R. S. McLean, M. D. Groner, A. A. Dameron, S. M. George, *J. Appl. Phys.* **2009**, *106*, 023533.
[24] M. D. Groner, J. W. Elam, F. H. Fabreguette, S. M. George, *Thin Solid Films* **2002**, *413*, 186.
[25] R. L. Puurunen, *J. Appl. Phys.* **2005**, *97*, 121301.
[26] A. C. Dillon, A. W. Ott, J. D. Way, S. M. George, *Surf. Sci.* **1995**, *322*, 230.
[27] M. D. Groner, F. H. Fabreguette, J. W. Elam, S. M. George, *Chem. Mater.* **2004**, *16*, 639.
[28] A. W. Ott, J. W. Klaus, J. M. Johnson, S. M. George, *Thin Solid Films* **1997**, *292*, 135.
[29] M. Juppo, A. Rahtu, M. Ritala, *Chem. Mater.* **2002**, *14*, 281.
[30] M. Ritala, M. Leskela, E. Rauhala, P. Haussalo, *J. Electrochem. Soc.* **1995**, *142*, 2731.
[31] S. M. George, B. Yoon, A. A. Dameron, *Acc. Chem. Res.* **2009**, *42*, 498.
[32] T. Yoshimura, S. Tatsuura, W. Sotoyama, *Appl. Phys. Lett.* **1991**, *59*, 482.
[33] T. Yoshimura, S. Tatsuura, W. Sotoyama, A. Matsuura, T. Hayano, *Appl. Phys. Lett.* **1992**, *60*, 268.
[34] H.-I. Shao, S. Umemoto, T. Kikutani, N. Okui, *Polymer* **1997**, *38*, 459.
[35] A. Kubono, N. Yuasa, H.-L. Shao, S. Umemoto, N. Okui, *Thin Solid Films* **1996**, *289*, 107.
[36] N. M. Adamczyk, A. A. Dameron, S. M. George, *Langmuir* **2008**, *24*, 2081.
[37] Y. Du, S. M. George, *J. Phys. Chem. C* **2007**, *111*, 8509.
[38] M. Putkonen, J. Harjuoja, T. Sajavaara, L. Niinisto, *J. Mater. Chem.* **2007**, *17*, 664.
[39] A. Kim, M. A. Filler, S. Kim, S. F. Bent, *J. Am. Chem. Soc.* **2005**, *127*, 6123.
[40] J. S. Lee, Y.-J. Lee, E. L. Tae, Y. S. Park, K. B. Yoon, *Science* **2003**, *127*, 818.

[41] P. W. Loscutoff, H. Zhou, S. B. Clendenning, S. F. Bent, *ACS Nano* **2010**, *4*, 331.
[42] P. W. Loscutoff, H.-B.-R. Lee, S. F. Bent, *Chem. Mater.* **2010**, *22*, 5563.
[43] Y. Li, D. Wang, J. M. Buriak, *Langmuir* **2010**, *26*, 1232.
[44] A. Kubono, N. Okui, *Prog. Polym. Sci.* **1994**, *19*, 389.
[45] S. M. George, B. H. Lee, B. Yoon, A. I. Abdulagatov, R. A. Hall, *J. Nanosci. Nanotechnol.* **2011**, *11*, 7956.
[46] A. A. Dameron, D. Seghete, B. B. Burton, S. D. Davidson, A. S. Cavanagh, J. A. Bertrand, S. M. George, *Chem. Mater.* **2008**, *20*, 3315.
[47] Q. Peng, B. Gong, R. M. VanGundy, G. N. Parsons, *Chem. Mater.* **2009**, *21*, 820.
[48] B. Yoon, J. L. O'Patchen, D. Seghete, A. S. Cavanagh, S. M. George, *Chem. Vap. Deposition* **2009**, *15*, 112.
[49] D. Seghete, R. A. Hall, B. Yoon, S. M. George, *Langmuir* **2010**, *26*, 19045.
[50] B. Yoon, D. Seghete, A. S. Cavanagh, S. M. George, *Chem. Mater.* **2009**, *21*, 5365.
[51] K. B. Klepper, O. Nilsen, P.-A. Hansen, H. Fjellvag, *Dalton Trans.* **2011**, *40*, 4036.
[52] K. B. Klepper, O. Nilsen, H. Fjellvag, *Dalton Trans.* **2010**, *39*, 11628.
[53] B. H. Lee, M. K. Ryu, S. Choi, K. H. Lee, S. Im, M. M. Sung, *J. Am. Chem. Soc.* **2007**, *129*, 16034.
[54] B. H. Lee, K. H. Lee, S. Im, M. M. Sung, *J. Nanosci. Nanotechnol* **2009**, *9*, 6962.
[55] B. H. Lee, K. H. Lee, S. Im, M. M. Sung, *Org. Electron.* **2008**, *9*, 1146.
[56] B. H. Lee, K. K. Im, K. H. Lee, S. Im, M. M. Sung, *Thin Solid Films* **2009**, *517*, 4056.
[57] B. H. Lee, B. Yoon, V. R. Anderson, S. M. George, *J. Phys. Chem. C* **2012**, *116*, 3250.
[58] T. Bitzer, N. V. Richardson, *Appl. Phys. Lett.* **1997**, *71*, 662.
[59] S. Haq, N. V. Richardson, *J. Phys. Chem. B* **1999**, *103*, 5256.
[60] B. G. Frederick, N. V. Richardson, W. N. U. A. E. Farrash, *Surf. Interface Anal.* **1993**, *20*, 434.
[61] X. Liang, D. M. King, P. Li, S. M. George, A. W. Weimer, *AIChE J.* **2009**, *55*, 1030.
[62] X. Liang, M. Yu, J. Li, Y.-B. Jiang, A. W. Weimer, *Chem. Commun.* **2009**, 7140.
[63] M. Yu, H. H. Funke, R. D. Noble, J. L. Falconer, *J. Am. Chem. Soc.* **2011**, *133*, 1748.
[64] R. A. Hall, S. M. George, unpublished.
[65] S. K. Kim, C. S. Hwang, S.-H. K. Park, S. J. Yun, *Thin Solid Films* **2005**, *478*, 103.
[66] J. W. Elam, Z. A. S. S. M. George, *Thin Solid Films* **2002**, *414*, 43.
[67] B. Yoon, B. H. Lee, S. M. George, *ECS Trans.* **2011**, *41*, 271.
[68] B. Yoon, Y. Lee, D. Derk, C. B. Musgrave, S. M. George, *ECS Trans.* **2011**, *33*, 191.
[69] C. K. Chiang, C. R. Fincher, Y. W. Park Jr., A. J. Heeger, H. Shirakawa, E. J. Louis, S. C. Gau, A. G. MacDiarmid, *Phys. Rev. Lett.* **1977**, *39*, 1098.
[70] S. Cho, G. Han, K. Kim, M. M. Sung, *Angew. Chem. Int. Ed.* **2011**, *50*, 2742.
[71] A. I. Abdulagatov, R. A. Hall, J. L. Sutherland, B. H. Lee, A. S. Cavanagh, S. M. George, *Chem. Mater.* **2012**, *24*, 2854.
[72] A. L. Linsebigler, G. Lu, J. T. Yates, *Chem. Rev.* **1995**, *95*, 735.
[73] B. H. Lee, V. R. Anderson, S. M. George, *ECS Trans.* **2011**, *41*, 131.
[74] J. P. Chang, Y. S. Lin, S. Berger, A. Kepten, R. Bloom, S. Levy, *J. Vac. Sci. Technol. B* **2001**, *19*, 2137.
[75] R. A. Synowicki, T. E. Tiwald, *Thin Solid Films* **2004**, *455*, 248.
[76] B. H. Lee, S. M. George, unpublished.
[77] T. M. Phung, J. M. Jensen, D. C. Johnson, J. J. Donovan, B. G. McBurnett, *X-Ray Spectrom.* **2008**, *37*, 608.
[78] Y. Y. Huang, A. Sarkar, P. C. Schultz, *J. Non-Cryst. Solids* **1977**, *27*, 29.
[79] W. C. Oliver, G. M. Pharr, *J. Mater. Res.* **2004**, *19*, 3.
[80] D. L. Joslin, W. C. Oliver, *J. Mater. Res.* **1990**, *5*, 123.
[81] D. C. Miller, R. R. Foster, S. Jen, J. A. Bertrand, D. Seghete, B. Yoon, Y. Lee, S. M. George, M. L. Dunn, *Acta Mater.* **2009**, *57*, 5083.
[82] K. Tapily, J. E. Jakes, D. S. Stone, P. Shrestha, D. Gu, H. Baumgart, A. A. Elmustafa, *J. Electrochem. Soc.* **2008**, *155*, H545.
[83] M. K. Tripp, C. Stampfer, D. C. Miller, T. Helbling, C. F. Herrmann, C. Hierold, K. Gall, S. M. George, V. M. Bright, *Sens. Actuators A* **2006**, *130-131*, 419.
[84] J. W. Elam, D. Routkevitch, S. M. George, *J. Electrochem. Soc.* **2003**, *150*, G339.
[85] T. L. Yang, D. H. Zhang, J. Ma, H. L. Ma, Y. Chen, *Thin Solid Films* **1998**, *326*, 60.
[86] U. Bach, D. Lupo, P. Comte, J. E. Moser, F. Weissortel, J. Salbeck, H. Spreitzer, M. Gratzel, *Nature* **1998**, *395*, 583.
[87] W. Gopel, K. D. Schierbaum, *Sens. Actuators B* **1995**, *26*, 1.
[88] N. Yamazoe, *Sens. Actuators B* **1991**, *5*, 7.
[89] S. L. Brock, N. G. Duan, Z. R. Tian, O. Giraldo, H. Zhou, S. L. Suib, *Chem. Mater.* **1998**, *10*, 2619.
[90] E. A. Mamedov, V. C. Corberan, *Appl. Catal. A* **1995**, *127*, 1.
[91] J. Q. Xi, M. F. Schubert, J. K. Kim, E. F. Schubert, M. F. Chen, S. Y. Lin, W. Liu, J. A. Smart, *Nat. Photonics* **2007**, *1*, 176.
[92] L. Han, P. Mandlik, J. Gartside, S. Wagner, J. A. Silvernail, R. Q. Ma, M. Hack, J. J. Brown, *J. Electrochem. Soc.* **2009**, *156*, H106.
[93] T. W. Kim, M. Yan, G. Erlat, P. A. McConnelee, M. Pellow, J. Deluca, T. P. Feist, A. R. Duggal, M. Schaepkens, *J. Vac. Sci. Technol. A* **2005**, *23*, 971.
[94] J. R. Cho, D. Y. Ha, *Mater. Sci. Eng. A* **2002**, *334*, 147.
[95] K. S. Ravichandran, *Mater. Sci. Eng. A* **1995**, *201*, 269.
[96] N. Cordero, J. Yoon, Z. G. Suo, *Appl. Phys. Lett.* **2007**, *90*, 111910.